Sustainable Energy & Fuels

PERSPECTIVE

View Article Online
View Journal | View Issue

Cite this: *Sustainable Energy Fuels*, 2018, **2**, 538

How to determine optical gaps and voltage losses in organic photovoltaic materials

K. Vandewal, †* J. Benduhn and V. C. Nikolis

Received 15th December 2017
Accepted 2nd February 2018

DOI: 10.1039/c7se00601b

rsc.li/sustainable-energy

The best performing organic solar cells (OSC) efficiently absorb photons and convert them to free charge carriers, which are subsequently collected at the electrodes. However, the energy lost in this process is much larger than for inorganic and perovskite solar cells, currently limiting the power conversion efficiency of OSCs to values slightly below 14%. To quantify energy losses, the open-circuit voltage of the solar cell is often compared to its optical gap. The latter is, however, not obvious to determine for organic materials which have broad absorption and emission bands, and is often done erroneously. Nevertheless, a deeper understanding of the energy loss mechanisms depends crucially on an accurate determination of the energies of the excited states involved in the photo-conversion process. This perspective therefore aims to summarize how the optical gap can be precisely determined, and how it relates to energy losses in organic photovoltaic materials.

Introduction

In the past 15 years, the power conversion efficiency (PCE) of organic solar cells (OSCs) has increased from about 1% to now almost 14%.[1] This development has been accomplished by the synthesis of new electron donating and electron accepting materials of which high performing combinations have been discovered. The highest external quantum efficiencies (EQE_{PV}) exceed 80%,[2] and fill-factors (FF) approach 80%,[3] being on-par with those of higher efficiency technologies, such as gallium arsenide (GaAs) and crystalline silicon (c-Si). Up to now, it is the open-circuit voltage of OSCs (V_{OC}) which is lagging behind, making OSCs currently still less efficient than established inorganic photovoltaic technology or the emerging perovskite solar cells. Therefore, research is nowadays focusing on the identification of the elementary processes responsible for the large difference between eV_{OC} and the optical gap of the main absorber (E_{opt}), where e is the elementary charge. At the same time, new materials are being synthesized,[4] as well as new device architectures have been developed,[5] with the aim to minimize these voltage losses.

Under solar illumination, the total energy loss per absorbed photon is equal to the difference between the photon energy and the product of e with the voltage at the point of maximum electrical power output. A lower limit for these energy losses is given by the difference between the device's optical gap (E_{opt}) and eV_{OC}. Indeed, the potential energy of the extracted charge carriers is limited to eV_{OC}, while E_{opt} is given by the lowest energy singlet exciton, either of the donor (E_{D^*}) or the acceptor (E_{A^*}). For the remainder of this perspective, we refer to $E_{opt}/e - V_{OC}$ as "voltage loss".

To precisely characterize and study energy and voltage loss mechanisms for OSCs, an accurate determination of the energies of the relevant electronic states in organic semiconductors is crucial. Following photon absorption, several electron-transfer steps introduce energy losses. Fig. 1 depicts the energy levels of singlet and triplet states on the neat donor (D) and acceptor (A) in a Jablonski diagram. Following electron transfer, an intermolecular charge-transfer (CT) state, comprising an electron on the acceptor and a hole on the donor, is formed. This state can decay to the ground state or dissociate into a state comprising fully free charge carriers (FC).

The energy and voltage losses in OSCs relate to the chemical potential of the free charge carriers under solar illumination, which is determined by the energies of the relevant excited states, as well as the transition rates between these states and the ground state. However, the excited state energies are often empirically determined. For example, CT state energies are sometimes estimated by taking the difference between the energy of the highest occupied molecular orbital of the donor, HOMO(D), and lowest unoccupied molecular orbital of the acceptor, LUMO(A). This approach however, neglects polarization and binding energies,[6] and values for the driving force for electron transfer can be over- or underestimated by several tenths of electron volts (eV). The singlet energies $E_{A^*(S1)}$ or $E_{D^*(S1)}$ of acceptor and donor, of which the lowest one can be considered as the optical gap (E_{opt}) of the blend, are often taken as the onset of the absorption spectrum, which is rather ill-defined. It is clear that further progress in the

Dresden Integrated Center for Applied Physics and Photonic Materials (IAPP), Institute for Applied Physics, Technische Universität Dresden, Nöthnitzer Straße 61, 01187 Dresden, Germany. E-mail: koen.vandewal@iapp.de

† Current address: Instituut voor Materiaalonderzoek (IMO), Hasselt University, Wetenschapspark 1, BE-3590, Diepenbeek, Belgium, E-mail: koen.vandewal@uhasselt.be.

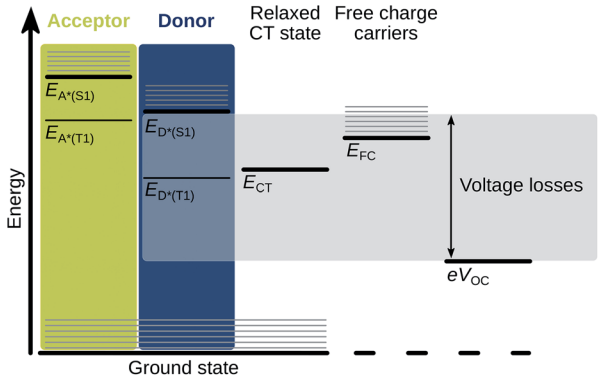

Fig. 1 Jablonski diagram, showing the energy levels which are important for OSCs. The lowest optical excitations in the absorber molecules, *i.e.* A and D, are singlet excitons ($E_{A^*(S1)}$ and $E_{D^*(S1)}$). The optical transition from the ground state to the triplet excited state ($E_{A^*(T1)}$ and $E_{D^*(T1)}$) are forbidden. The intermolecular CT state between D and A has the energy E_{CT}. In OSCs, charge generation and recombination takes place *via* this state, therefore, we can define voltage losses with respect to this state, or with respect to the strongly absorbing singlet states on the neat materials. The energy difference between the lowest energy singlet exciton and eV_{OC} forms a lower limit for the energy lost in the conversion of strongly absorbed photons to charges collected at the electrodes.

fundamental understanding of OSC operation needs an unambiguous method to determine voltages losses, so that they can be compared between research groups. This perspective aims therefore to summarize how optical gaps and CT state energies can be consistently determined and how they relate to voltage losses in OSCs.

Absorption, emission and the optical gap

Spectral broadening in organic materials

For a hypothetical solar cell with an ideal step-wise absorption spectrum, determination of E_{opt} is trivial, as it corresponds to the lowest energy for which photons are strongly absorbed. In reality, OSCs exhibit rather shallow absorption tails, due to the presence of static and dynamic disorder, as well as the presence of weakly absorbing CT states. In order to unambiguously determine E_{opt}, it is instructive to consider the origins of the spectral broadening.

The absorption and emission spectra of organic materials are strongly affected by electron–phonon coupling and molecular vibrations. Fig. 2a shows how the high frequency vibrations, for example ring breathing modes, are responsible for discrete peaks in the spectra.[7] For these high frequency modes the spacing between the vibrational energy levels is much larger than the thermal energy and electrons populate solely the lowest energy vibrational level $\nu = 0$. Photon absorption and emission solely occurs for discrete photon energies related to transitions between a vibrational level of the ground state ν, and a vibrational level of the excited state ν'. The 0–0 transition occurs at the energy $E_{0\text{–}0}$, which is the difference between vibrationally relaxed ground- and excited state.

However, the absorption and emission spectra of organic thin films seldom consist of well resolved, discrete peaks: a main source of peak broadening are low frequency vibrations with an energy spacing less than the thermal energy (Fig. 2b).[7] Optical transitions from thermally (Boltzmann) populated low frequency vibrational modes result in absorption at photon energies below $E_{0\text{–}0}$ and emission at photon energies above $E_{0\text{–}0}$. Treating the low frequency vibrations as harmonic oscillators results in Gaussian absorption ($A(E)$) and emission ($N(E)$) lineshapes

$$A(E) \sim E \exp\left(-\frac{(E - E_{0\text{–}0} - \lambda_L)^2}{4\lambda_L k_B T}\right) \quad (1)$$

$$N(E) \sim E^3 \exp\left(-\frac{(E - E_{0\text{–}0} + \lambda_L)^2}{4\lambda_L k_B T}\right) \quad (2)$$

hereby, E corresponds to the photon energy and k_B is the Boltzmann constant. The line-width is proportional to the temperature T and the low frequency relaxation energy λ_L. The energy difference between vibrational relaxed ground- and excited state, $E_{0\text{–}0}$, is the crossing point of the appropriately normalized absorption and emission spectra, as shown in Fig. 2b.

Extracting singlet and charge-transfer state energies

In what follows, we outline how eqn (1) and (2) can be used to accurately extract the energy levels $E_{D^*(S1)}$ or $E_{A^*(S1)}$ and E_{CT} for OSC blends. Hereby, we consider that the absorption spectrum of a donor–acceptor blend for OSCs will be mainly determined by high oscillator strength optical transitions on the neat materials. However, within their gap, much weaker absorption related to direct excitation of CT states is present. The optical gap (E_{opt}) is identified as the $E_{0\text{–}0}$ transition energy of the singlet localized on either donor or acceptor. The $E_{0\text{–}0}$ of the CT state (E_{CT}) is often lower than E_{opt}. Both E_{opt} and E_{CT} can be determined from the optical spectra by a fit of the low energy absorption tail or high energy emission tail with eqn (1) or (2), respectively. Alternatively, one can make use of the fact that $E_{0\text{–}0}$ coincides with the energy at which the appropriately normalized absorption and emission spectrum cross. Dividing $A(E)$ by E and $N(E)$ by E^3, yields the so-called reduced absorption and emission spectra. When normalizing the reduced spectra to the maximum of the corresponding peak, eqn (1) and (2) intersect exactly at $E = E_{0\text{–}0}$. In the case of mirror-image spectra, $E_{0\text{–}0}$ is the midpoint between the absorption and emission maxima (Stokes shift), separated by $2\lambda_L$.[8]

As a concrete example, Fig. 3a shows the determination of E_{opt} ($E_{D^*(S1)}$) and E_{CT} for vacuum-processed OSCs based on ZnPc:C_{60} and F_4ZnPc:C_{60} active layers. Photovoltaic diodes comprising both neat donors and their blends with C_{60} were fabricated. The electroluminescence (EL) and photovoltaic external quantum efficiency (EQE_{PV}) spectra of these diodes were measured and provide a reliable measurement of the emission and absorption tails. It should be noted that EQE_{PV} and absorption spectra are interchangeable here, since the

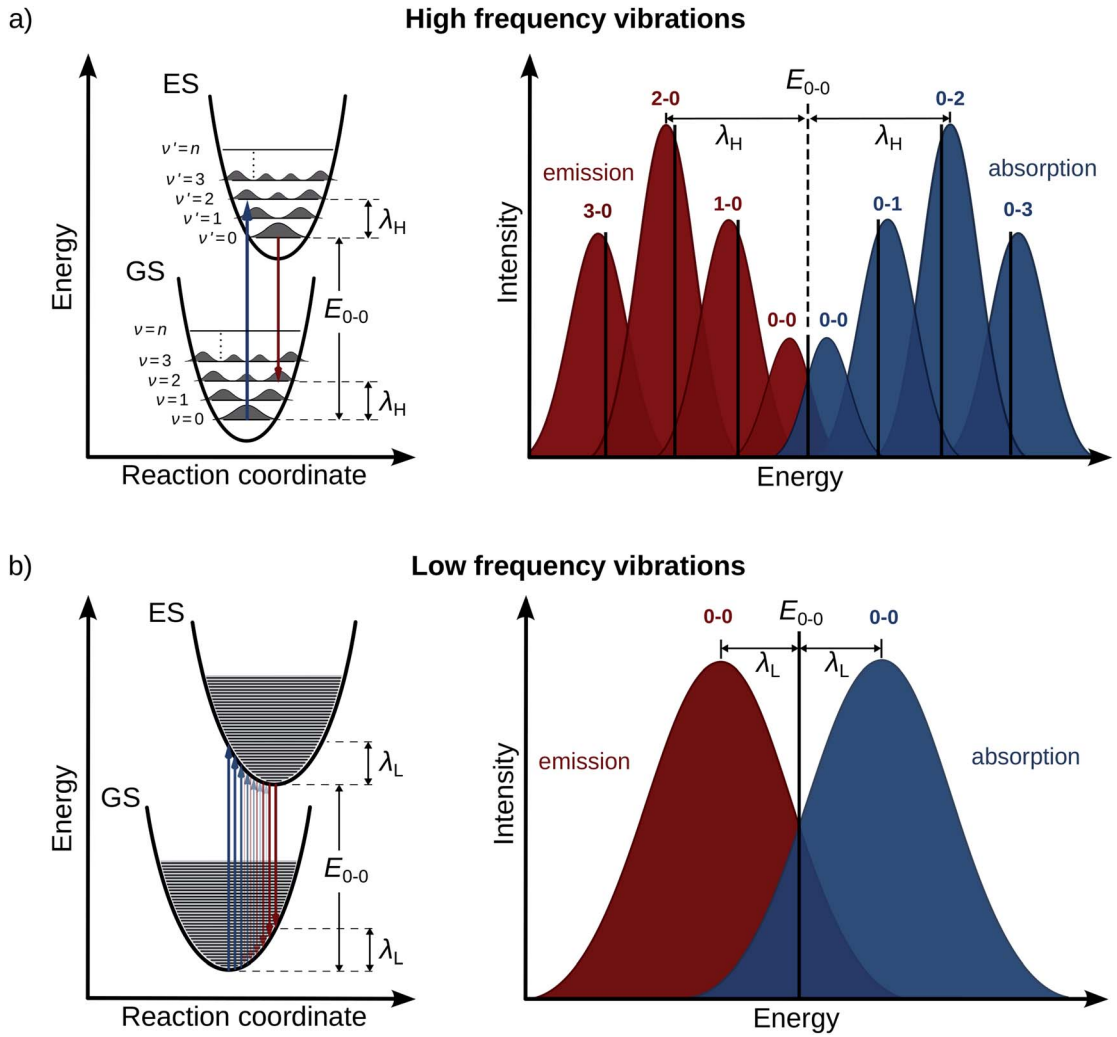

Fig. 2 Optical transitions depicted in an energy diagram with displaced potential wells for the ground state (GS) and excited state (ES), taking into account that the reaction coordinate remains invariant during the transition (Franck–Condon principle). Vertical blue arrows represent absorption and vertical red arrows emission. (a) Absorption and emission spectra are dominated by high frequency vibrations, with a relaxation energy λ_H. In this case, the spacing between vibrational levels is larger than the thermal energy. Photon absorption occurs by promoting an electron from the vibrational ground state level $\nu = 0$ to an excited state vibrational level ν', indicated by the black lines in the corresponding absorption spectrum. In the emission spectrum, transitions from the lowest excited state vibrational level $\nu' = 0$ to ground state levels ν dominate, as indicated by the black lines in the emission spectra. Absorption and emission spectra overlap around the 0–0 transition energy (E_{0-0}). (b) Peak broadening by low frequency vibrations with reorganization energy λ_L. The spacing between vibrational levels is less than the thermal energy. Optical transitions from higher energy thermally populated levels results in absorption at photon energies below E_{0-0} and emission at energies above E_{0-0}. The resulting peak width depends on temperature and λ_L.

internal quantum efficiency (IQE) of D:A photovoltaic blends is rather constant at their low energy tail.[9] Furthermore, EL spectra were measured at low injection currents, keeping the system in quasi-equilibrium.[9] For the neat phthalocyanines, the crossing point between the normalized reduced absorption (EQE_{PV}) and reduced emission (EL) spectra yields a similar value for E_{opt} ($E_{D^*(S1)}$) around 1.52–1.53 eV. For the blends with C_{60}, reduced EQE_{PV} and EL curves are plotted on a logarithmic scale, on which for ZnPc:C_{60}, an additional CT absorption band becomes visible. The EL spectrum of the blend is dominated by CT emission. Fits of EQE_{PV} and EL with respectively eqn (1) and (2) yield similar values for E_{CT}, which coincide rather well with the crossing point of the spectra at 1.17 eV. Fluorination of the phthalocyanine donor leads to a decrease of both its HOMO and LUMO. Therefore, we observe a blue-shift of the CT absorption band for F_4ZnPc:C_{60} blend as compared to ZnPc:C_{60}. In fact, the CT absorption becomes indistinguishable from the neat F_4ZnPc absorption tail. A fit of the EL spectrum with eqn (2) and the crossing point between reduced EL and EQE_{PV} yield an E_{0-0} energy of 1.46 eV, *i.e.* 60 meV lower than the E_{opt} of F_4ZnPc. In this case optical transitions related to CT state excitation and low energy F_4ZnPc excitation are indistinguishable.

With the knowledge of E_{opt} and E_{CT} for both material systems, we can now perform a detailed analysis of the voltage losses, summarized in Fig. 3c and f. The V_{OC} was measured under

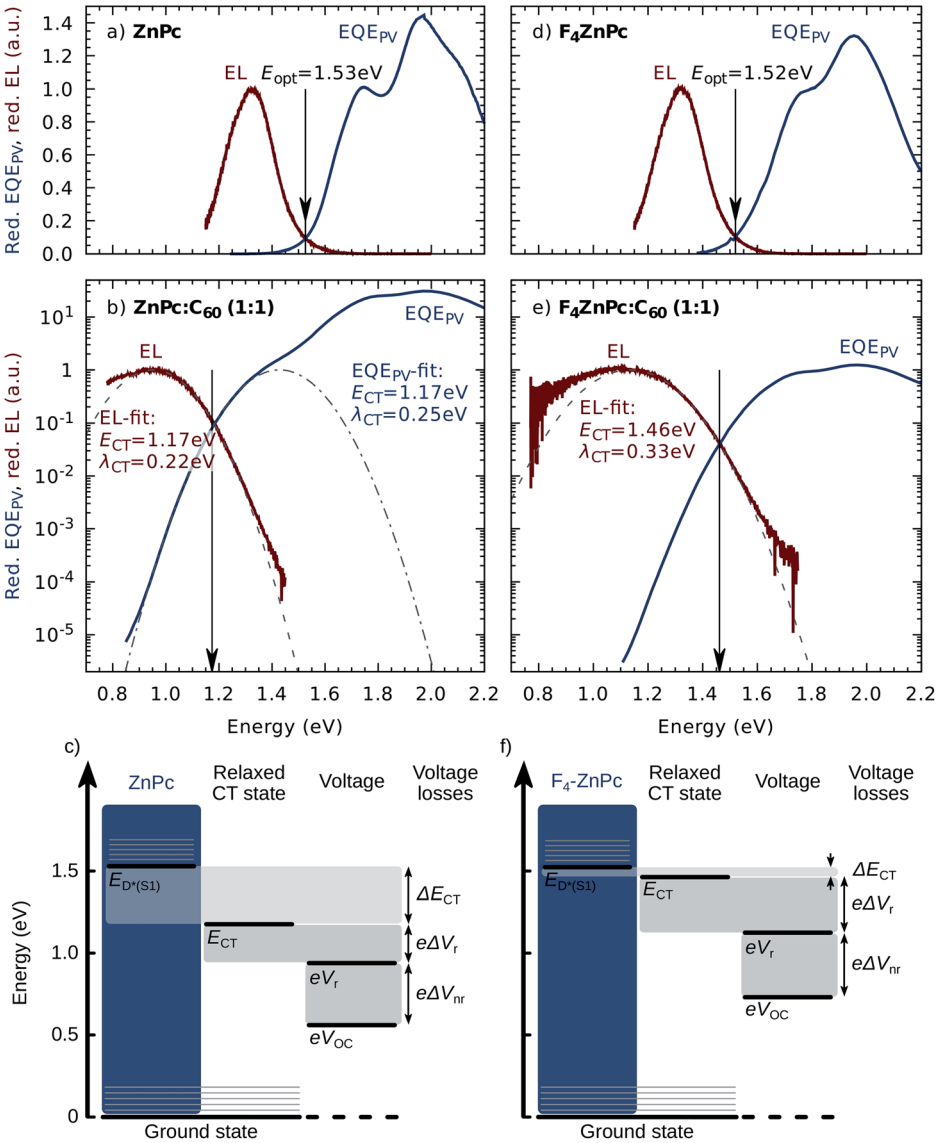

Fig. 3 Examples of determining the E_{opt} and E_{CT} for 2 different OSCs: (a) neat ZnPc, (b) ZnPc:C_{60} and (d) neat F_4ZnPc, (e) F_4ZnPc:C_{60}. In every sub-figure, the black arrow shows the position of the crossing point between reduced and normalized EQE_{PV} and EL spectra. (c) and (f) summarize the voltage losses in the two exemplary devices. The E_{opt} of the donor and E_{CT} of the blend are obtained as described in the main text, V_r is calculated from the EQE_{PV} spectra, and V_{OC} is measured at 1 sun illumination for the corresponding device. Further details on the voltage losses are given in the main text.

simulated solar illumination for both ZnPc:C_{60} (V_{OC} = 0.56 V) and F_4ZnPc:C_{60} (V_{OC} = 0.73 V) with the latter being 0.17 V higher.

The conversion of the lowest energy singlet excited state on the donor to a free electron–hole pair with a chemical potential eV_{OC} occurs at the cost of ΔE_{loss}, given by

$$\Delta E_{loss} = E_{opt} - eV_{OC} \quad (3)$$

The associated voltages losses $\Delta V_{loss} = \Delta E_{loss}/e$ are 0.97 V for ZnPc:C_{60} and 0.79 V for F_4ZnPc:C_{60}. The lower loss for F_4ZnPc:C_{60} is largely due to a reduced energy loss in the charge-transfer process, converting a relaxed phthalocyanine singlet exciton to a relaxed CT state.

$$\Delta E_{CT} = E_{opt} - E_{CT} \quad (4)$$

While the electron transfer process in ZnPc:C_{60} is accompanied by a ΔE_{CT} of 0.36 eV, this loss is only 0.06 eV in F_4ZnPc:C_{60}, and the absorption and emission tails for blend and neat F_4ZnPc almost coincide. Here, we want to emphasize that the optical determination of ΔE_{CT}, as described above, is a much more accurate way of determining the "driving force" for charge transfer as simply taking the LUMO(D)–LUMO(A) or HOMO(A)–HOMO(D) difference, which ignores exciton binding and polarization energies. Indeed, in the initial photo-induced electron transfer event, donor (or acceptor) excitons, with minimum energy (E_{opt}) are converted to CT states, with energy E_{CT}. Seeing this process as free electrons (holes) in the LUMO(D)

(HOMO(A)), converted to free electrons (holes) in the LUMO(A) (LUMO(D)) would certainly be wrong.

The chemical potential at open-circuit conditions, eV_{OC} is lower as compared to E_{CT} due to recombination of free charge carriers.

$$\Delta V_{rec} = \frac{1}{e}E_{CT} - V_{OC} \quad (5)$$

For ZnPc:C_{60}, the recombination loss ΔV_{rec} is 0.61 V while for F_4ZnPc:C_{60} the total voltage loss is almost fully due to recombination. In general, recombination losses often comprise a substantial fraction of the total voltage losses in OSCs and are often found to be around 0.6 V, when V_{OC} is measured at room temperature and under 1 sun illumination.[10,11]

To understand the origin of the recombination caused voltage losses in more detail, it is useful to consider the influence of radiative and non-radiative recombination on V_{OC} separately. When only radiative recombination would occur, V_{OC} would reach its upper limit, the so-called V_r, which can be calculated as:[12,13]

$$V_r = \frac{k_B T}{q} \ln \frac{J_{SC}}{J_0^r} \quad (6)$$

where J_{SC} is the short-circuit current density obtained by integrating the product of the EQE_{PV} spectrum and the solar AM1.5G spectrum, and J_0^r is the radiative limit of the dark current, obtained by integrating the product of the EQE_{PV} spectrum and black body spectrum at room temperature. More details on this procedure, which assumes thermal equilibrium between CT states and free charge carriers, can be found in ref. 13.

Voltage losses due to radiative recombination, ΔV_r are given by

$$\Delta V_r = \frac{1}{e}E_{CT} - V_r \quad (7)$$

They are in a sense fundamental, because they are a direct consequence of the fact that OSCs absorb light.[14] From the available sensitively measured EQE_{PV} spectra we calculate a V_r of 0.93 V for ZnPc:C_{60} and a V_r of 1.12 V for F_4ZnPc:C_{60}, corresponding to $\Delta V_r = 0.24$ V and $\Delta V_r = 0.34$ V, respectively. The latter radiative losses are higher due to stronger absorption of the radiatively recombining species in F_4ZnPc:C_{60}.

The difference between the radiative limit of the V_{OC}, the V_r, and the in reality measured V_{OC} corresponds to non-radiative voltage losses, ΔV_{nr}

$$\Delta V_{nr} = V_r - V_{OC} \quad (8)$$

They are caused by due to non-radiative decay processes. It has been shown theoretically and experimentally that:

$$\Delta V_{nr} = \frac{k_B T}{e} \ln\left(EQE_{EL}^{-1}\right) \quad (9)$$

With EQE_{EL} being the quantum yield of radiative decay, which is the ratio of the radiative recombination rate to the total sum of radiative and non-radiative recombination rate. To determine ΔV_{nr} *via* a measurement of EQE_{EL} one should take care that the applied injection current is low, so that quasi-equilibrium conditions are ensured and the charge density in the device corresponds to that under solar conditions. For ZnPc:C_{60} and F_4ZnPc:C_{60} these ΔV_{nr} are 0.38 V and 0.39 V, respectively. In both cases, this is a substantial part of the total recombination losses, corresponding to an EQE_{EL} of about 3×10^{-7}, which is a low value as compared to other photovoltaic technologies. The resulting large non-radiative voltage losses have been proposed to be intrinsic for fullerene OSCs, limiting their maximum achievable power conversion efficiency.[11]

Temperature and illumination intensity dependence of the voltage losses

For an analysis of the voltage losses, one should keep in mind that V_{OC} is temperature and illumination intensity dependent. Most expressions for V_{OC} are of the general form:[15]

$$V_{OC} = V_0 - \beta T \ln(J_{ph}) \quad (10)$$

hereby is J_{ph} the photocurrent density and β a temperature and light intensity independent parameter. The extrapolation of temperature dependent V_{OC} measurements to 0 K leads to V_0 and delivers β, which depends on the details of the free carrier recombination processes.

For OSCs, V_0 has been found to correspond to E_{CT}, rather than HOMO(D)–LUMO(A).[13,16] It has been shown that this is due to the fact that the CT states are in thermal equilibrium with the free charge carriers.[17,18] As a result, the total recombination losses ΔV_{rec}, radiative and non-radiative, are temperature dependent. Besides the optical method described above, temperature dependent measurements of V_{OC} therefore provide and an alternative method to determine E_{CT} and the recombination losses.

Even when static disorder is present, the absorption and emission tails which are already broadened by electron–phonon coupling are additionally broadened by the site energy spread. When fitting EQE_{PV} and EL with eqn (1) and (2), this will result in a temperature dependent E_{CT}. However, the extrapolation of V_{OC} to 0 K will still correspond to the extrapolation of E_{CT} to 0 K.[17] Therefore, the optical method of determining E_{CT} and the temperature dependent V_{OC} method are consistent with each other.[13]

Minimizing energy losses for strongly absorbed photons

To finalize this perspective, we summarize some of the characteristics which benefit low-voltage-loss OSCs. As exemplified by the ZnPc:C_{60} and F_4ZnPc:C_{60} systems, increasing E_{CT} to minimize ΔE_{CT} can be done by chemical design, controlling the frontier energy levels of donor and acceptor. For several new donor–acceptor combinations for OSCs, ΔE_{CT} is vanishingly

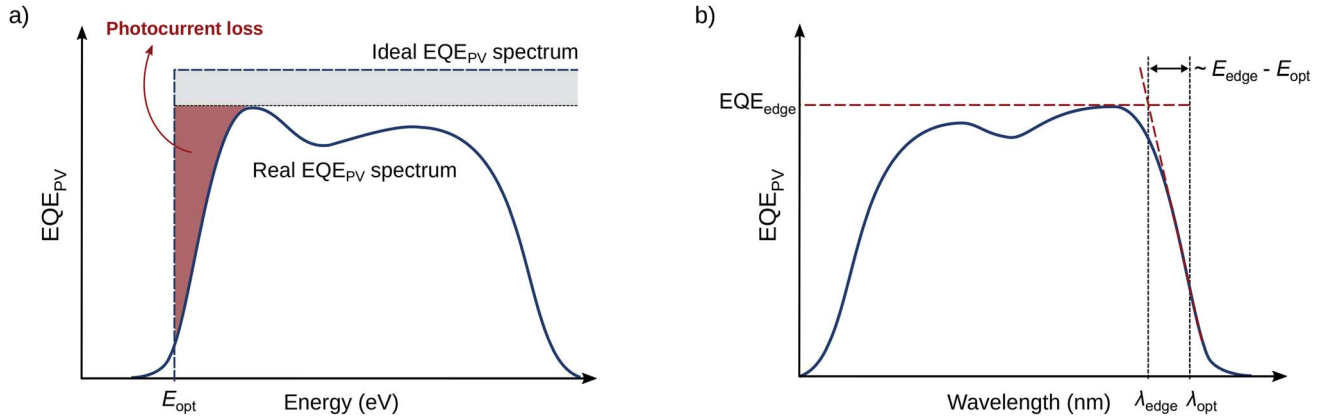

Fig. 4 (a) An ideal step-wise EQE_{PV} spectrum and an exemplary real EQE_{PV} spectrum, exhibiting a shallow absorption edge, for a hypothetical OSC. Optical and transport losses reduce the maximum obtainable EQE_{PV} of solar cells (grey area). The shallow absorption edge induces low EQE_{PV} for photons with energy just above E_{opt}. For a steep absorption edge, this photocurrent loss is minimized. (b) Graphical determination of λ_{edge} as the intersection of the extrapolated linear part of the absorption edge, and the isoline passing through the peak at the low-energy edge (EQE_{edge}) of the EQE_{PV} spectrum. E_{edge} corresponds to the energy of the absorbed low-energy photons which highly contribute to the device's photocurrent, and is obtained as $1240/\lambda_{edge}$ (nm). Considering energy losses from eV_{OC} to E_{edge} takes into account the steepness of the absorption edge, and promotes solar cells exhibiting E_{edge} close to E_{opt}. Here, λ_{opt} is the wavelength associated with E_{opt} as $\lambda_{opt} = 1240/E_{opt}$ (eV). With known E_{opt}, the offset $E_{edge} - E_{opt}$ is a measure of the absorption edge steepness. Efficient solar cell performance requires the lowest $E_{edge} - eV_{OC}$ difference at the highest possible EQE_{edge}.

small, while still high EQE_{PV} values can be achieved.[5,19,20] In those cases, the recombination losses ΔV_{rec} are the dominant ones. Up to now, only few strategies to suppress these losses have been proposed, including the suppression of the donor–acceptor interfacial area to reduce ΔV_r,[21–23] and the use of a cascaded device architecture, suppressing partly ΔV_{nr}.[5]

It is however important to note that even if the voltage losses $E_{opt} - eV_{OC}$ are minimized, this does not necessarily mean that the solar cell will be highly efficient. Complementary to a high V_{OC}, a high PCE requires also high photocurrent and FF. For this to be the case, charge generation and extraction has to be efficient at low ΔE_{CT} and the EQE_{PV} needs to be high (near unity) for all photons with an energy higher than E_{opt}. However, the shallow absorption edge of organic materials results in low EQE_{PV} for photon energies close to E_{opt} (see Fig. 4a).

We have recently introduced a metric which takes this into account and considers voltage losses for strongly absorbed photons, at the low-energy tail of the EQE_{PV} spectrum, as the difference $E_{edge} - eV_{OC}$.[5] Hereby, E_{edge} is defined as illustrated in Fig. 4b. For efficient solar cells, a low difference $E_{edge} - eV_{OC}$ at very high EQE_{edge} is required. Energy losses related to the steepness of the main absorber's absorption edge are quantified by $E_{edge} - E_{opt}$, implying that for OSCs exhibiting the desired steep absorption edge, the $E_{edge} - E_{opt}$ offset will be minimal. To keep these losses low, Fig. 2 shows that small low-frequency relaxation energies of the neat material excitons are required.

The determination of the voltage losses for strongly absorbed photons with this metric requires only standard EQE_{PV} and *J–V* measurements. This has the advantage that basically every photovoltaic device whose EQE_{PV} spectrum and *J–V* curve are known can be compared in terms of voltage losses. However, for a deeper physical insight and identification of the voltage limiting factors, exact determinations of E_{opt} and E_{CT} are essential.

Concluding statement

More systematic analysis of voltage losses of future donor–acceptor combinations for organic photovoltaics is required for a rigorous comparison between results and materials from different research groups. With this perspective, we encourage the reader not to use ill-defined absorption onsets, at which virtually no photons are absorbed, as reference point for voltage losses. Nor do we promote the use of HOMO and LUMO energy levels to determine the relevant energies of excited states in OSCs. The optical measurements described above, or temperature dependent measurements of V_{OC} contain much more useful and precise information. Finally, we would also like to encourage researchers working on the minimization of voltage losses in OSCs, to accompany claims of low voltage losses with a measurement of the EQE_{EL} (measured at an applied voltage similar to V_{OC}), since solar cells with truly low voltage losses will also be efficient LEDs.

Conflicts of interest

There are no conflicts to declare.

Acknowledgements

This work received funding from the German Federal Ministry for Education and Research (BMBF) through the InnoProfile Projekt “Organische p–i–n Bauelemente 2.2” (03IPT602X).

Notes and references

1 Y. Cui, H. Yao, B. Gao, Y. Qin, S. Zhang, B. Yang, C. He, B. Xu and J. Hou, *J. Am. Chem. Soc.*, 2017, **139**, 7302–7309.
2 W. Zhao, S. Li, H. Yao, S. Zhang, Y. Zhang, B. Yang and J. Hou, *J. Am. Chem. Soc.*, 2017, **139**, 7148–7151.
3 X. Guo, N. Zhou, S. J. Lou, J. Smith, D. B. Tice, J. W. Hennek, R. P. Ortiz, J. T. L. Navarrete, S. Li, J. Strzalka, L. X. Chen, R. P. H. Chang, A. Facchetti and T. J. Marks, *Nat. Photonics*, 2013, **7**, 825–833.
4 S. Li, W. Liu, C.-Z. Li, M. Shi and H. Chen, *Small*, 2017, **13**, 201701120.
5 V. C. Nikolis, J. Benduhn, F. Holzmueller, F. Piersimoni, M. Lau, O. Zeika, D. Neher, C. Koerner, D. Spoltore and K. Vandewal, *Adv. Energy Mater.*, 2017, **7**, 1700855.
6 J.-L. Bredas, *Mater. Horiz.*, 2014, **1**, 17–19.
7 A. Kohler and H. Bassler, *Electronic Processes in Organic Semiconductors: An Introduction*, Wiley-VCH Verlag GmbH & Co. KGaA, Weinheim, Germany, 2015, vol. 1.
8 R. A. Marcus, *J. Phys. Chem.*, 1989, **93**, 3078–3086.
9 K. Vandewal, S. Albrecht, E. T. Hoke, K. R. Graham, J. Widmer, J. D. Douglas, M. Schubert, W. R. Mateker, J. T. Bloking, G. F. Burkhard, A. Sellinger, J. M. J. Fréchet, A. Amassian, M. K. Riede, M. D. McGehee, D. Neher and A. Salleo, *Nat. Mater.*, 2014, **13**, 63–68.
10 K. R. Graham, P. Erwin, D. Nordlund, K. Vandewal, R. Li, G. O. Ngongang Ndjawa, E. T. Hoke, A. Salleo, M. E. Thompson, M. D. McGehee and A. Amassian, *Adv. Mater.*, 2013, **25**, 6076–6082.
11 J. Benduhn, K. Tvingstedt, F. Piersimoni, S. Ullbrich, Y. Fan, M. Tropiano, K. A. McGarry, O. Zeika, M. K. Riede, C. J. Douglas, S. Barlow, S. R. Marder, D. Neher, D. Spoltore and K. Vandewal, *Nat. Energy*, 2017, **2**, 17053.
12 U. Rau, *Phys. Rev. B: Condens. Matter Mater. Phys.*, 2007, **76**, 85303.
13 K. Vandewal, K. Tvingstedt, A. Gadisa, O. Inganäs and J. V. Manca, *Phys. Rev. B: Condens. Matter Mater. Phys.*, 2010, **81**, 125204.
14 P. Würfel and U. Würfel, *Physics of Solar Cells: From Basic Principles to Advanced Concepts*, Wiley-VCH Verlag GmbH & Co. KGaA, Weinheim, Germany, 2016.
15 M. A. Green, *Prog. Photovoltaics*, 2003, **11**, 333–340.
16 U. Hörmann, J. Kraus, M. Gruber, C. Schuhmair, T. Linderl, S. Grob, S. Kapfinger, K. Klein, M. Stutzman, H. J. Krenner and W. Brütting, *Phys. Rev. B: Condens. Matter Mater. Phys.*, 2010, **88**, 235307.
17 T. M. Burke, S. Sweetnam, K. Vandewal and M. D. McGehee, *Adv. Energy Mater.*, 2015, **5**, 1–12.
18 K. Vandewal, *Annu. Rev. Phys. Chem.*, 2016, **67**, 113–133.
19 N. A. Ran, J. A. Love, C. J. Takacs, A. Sadhanala, J. K. Beavers, S. D. Collins, Y. Huang, M. Wang, R. H. Friend, G. C. Bazan and T. Q. Nguyen, *Adv. Mater.*, 2016, **28**, 1482–1488.
20 J. Liu, S. Chen, D. Qian, B. Gautam, G. Yang, J. Zhao, J. Bergqvist, F. Zhang, W. Ma, H. Ade, O. Inganäs, K. Gundogdu, F. Gao and H. Yan, *Nat. Energy*, 2016, **1**, 16089.
21 K. Vandewal, J. Widmer, T. Heumueller, C. J. Brabec, M. D. McGehee, K. Leo, M. Riede and A. Salleo, *Adv. Mater.*, 2014, **26**, 3839–3843.
22 D. Credgington and J. R. Durrant, *J. Phys. Chem. Lett.*, 2012, **3**, 1465–1478.
23 M. A. Fusella, A. N. Brigeman, M. Welborn, G. E. Purdum, Y. Yan, R. D. Schaller, Y. L. Lin, Y.-L. Loo, T. Van Voorhis, N. C. Giebink and B. P. Rand, *Adv. Energy Mater.*, 2017, 1701494.

